

## Low-Energy Collective Oscillations and Bogoliubov Sound in an Exciton-Polariton Condensate

E. Estrecho<sup>1,\*</sup>, M. Pieczarka<sup>1,‡</sup>, M. Wurdack,<sup>1</sup> M. Steger,<sup>2,§</sup> K. West,<sup>3</sup> L. N. Pfeiffer,<sup>3</sup> D. W. Snoke,<sup>2</sup> A. G. Truscott,<sup>4</sup> and E. A. Ostrovskaya<sup>1,†</sup>

<sup>1</sup>ARC Centre of Excellence in Future Low-Energy Electronics Technologies & Nonlinear Physics Centre, Research School of Physics, The Australian National University, Canberra ACT 2601, Australia

<sup>2</sup>Department of Physics and Astronomy, University of Pittsburgh, Pittsburgh, Pennsylvania 15260, USA

<sup>3</sup>Department of Electrical Engineering, Princeton University, Princeton, New Jersey 08544, USA

<sup>4</sup>Laser Physics Centre, Research School of Physics, The Australian National University, Canberra ACT 2601, Australia



(Received 28 April 2020; revised 24 August 2020; accepted 28 January 2021; published 15 February 2021)

We report the observation of low-energy, low-momenta collective oscillations of an exciton-polariton condensate in a round “box” trap. The oscillations are dominated by the dipole and breathing modes, and the ratio of the frequencies of the two modes is consistent with that of a weakly interacting two-dimensional trapped Bose gas. The speed of sound extracted from the dipole oscillation frequency is smaller than the Bogoliubov sound, which can be partly explained by the influence of the incoherent reservoir. These results pave the way for understanding the effects of reservoir, dissipation, energy relaxation, and finite temperature on the superfluid properties of exciton-polariton condensates and other two-dimensional open-dissipative quantum fluids.

DOI: 10.1103/PhysRevLett.126.075301

**Introduction.**—Low-energy collective excitations directly probe Bogoliubov sound in quantum fluids and gases, which in turn provides critical information on the thermodynamic and superfluid properties of these systems. Propagation of sound in two-dimensional (2D) quantum fluids [1–5] is particularly interesting, since it is governed by Berezinskii-Kosterlitz-Thouless (BKT) rather than Bose-Einstein condensation (BEC) physics. Furthermore, collective excitations in 2D quantum gases can reveal quantum corrections to classical symmetries [6,7], and quantum phase transitions [8–10].

Two-dimensional nonequilibrium condensates of exciton polaritons (polaritons hereafter) [11–16] exhibit a wide range of phenomena including BKT [17–19] and Bardeen-Cooper-Schrieffer (BCS) [20–22] physics, as well as superfluidlike behavior [23–26]. Their collective excitation spectrum is complex, and is expected to differ from the Bogoliubov prediction for an equilibrium BEC, especially at small momenta, due to dissipation [27,28], coupling to an incoherent excitonic reservoir [29,30] and finite-temperature effects. Contrary to expectations, recent experiments [31–34] revealed an excitation spectrum consistent with Bogoliubov theory. However, these experiments either could not probe the low-momenta region of the excitation spectrum [32,33], or were performed in a near-equilibrium regime [34] without the influence of the reservoir. Hence, direct access to the low-energy excitations and their damping rates is needed to understand the influence of nonequilibrium and finite temperature effects on polariton superfluid dynamics.

In this Letter, we report the observation of low-energy collective oscillations of a trapped 2D polariton condensate. Using an optically induced round box trap in the pulsed excitation regime [35], we create an interaction-dominated condensate undergoing long-lived “sloshing” (Fig. 1). The frequency ratio of the two normal modes of the dynamics, i.e., center-of-mass (dipole) and breathing (monopole) oscillations, is in remarkable agreement with the theory for a weakly interacting 2D Bose gas in thermal equilibrium. However, the speed of sound extracted from the dipole mode frequency is lower than expected and has a nontrivial dependence on the interaction energy, pointing to a strong influence of the incoherent reservoir on the low-energy collective excitations.

**Experiment.**—The polaritons are created in a high-quality GaAs/AlAs  $3\lambda/2$  microcavity sandwiched between 32 (top) and 40 (bottom) pairs of distributed Bragg reflectors with 12 embedded GaAs quantum wells of nominal thickness 7 nm [36]. A high-density condensate is formed in an optically induced round trap [see Fig. 1(a)] using an off resonant pulsed excitation in a geometry similar to Ref. [35]. A spatial hole-burning effect [35,37] ensures that the pump-induced trapping potential is box-like, which is reflected by the sharp edges of the condensate density distribution in the Thomas-Fermi regime, see the Supplemental Material [38]. Time-resolved spectral imaging of real space (RS) and  $k$ -space (KS) dynamics is enabled by a streak camera. The condensate forms in  $\sim 50$  ps and then slowly decays, resulting in a fast rise and slow fall of the time-resolved photoluminescence (PL)

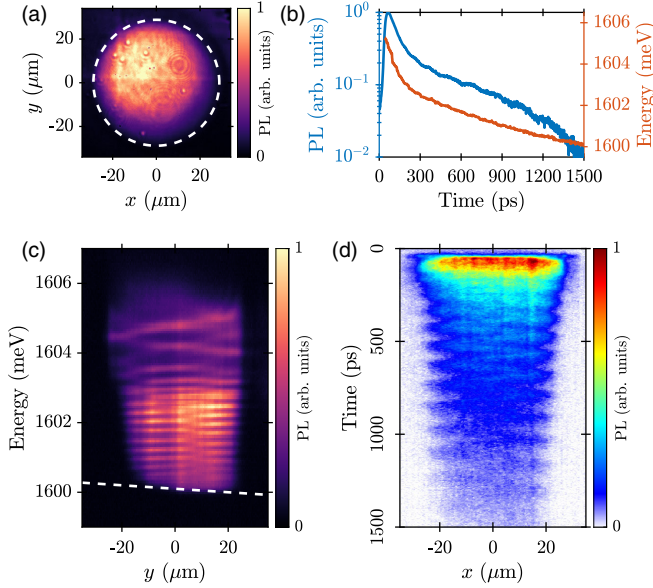


FIG. 1. Sloshing interaction-dominated polariton condensate. (a) Time-integrated real space image of the condensate trapped in a round box potential (dashed line) of the diameter  $D = 56 \mu\text{m}$ . (b) Time-resolved, spatially integrated, normalized PL intensity (blue) and the condensate energy (orange) measured at the center of the trap. (c) Time-integrated real space spectrum of the condensate along the  $y$  axis at  $x \approx 0$ . Dashed line is a guide to the eye indicating the tilted bottom of the optically induced potential. (d) Time-resolved real space distribution of the condensate along the  $x$  axis at  $y \approx 0$ .

signal, as shown in Fig. 1(b). Decay of the condensate density leads to decreasing energy blueshift  $\Delta E$  associated with the condensate, which results in one-to-one correspondence between time and the condensate energy.

The condensate usually decays on a timescale of the polariton lifetime ( $\sim 200$  ps), which makes it impossible to track the slow dynamics of collective oscillations. To overcome this limitation, we use a high-energy photoexcitation  $\sim 150$  meV above the lower polariton resonance, which produces a large reservoir with a very low effective decay rate [39] (see the Supplemental Material [38]). The lifetime of the condensate replenished by this reservoir is much greater than the polariton lifetime, as evidenced by the long PL decay time (up to 1.5 ns) [Fig. 1(b)]. This also results in a bright low-energy tail in the RS spectrum [see Fig. 1(c)]. Slow decay of the condensate is key to our measurement.

**Results.**—Time-integrated imaging of the condensate [e.g., Fig. 1(a)] typically washes out all dynamics. In this work, due to the well-defined time-resolved energy of the condensate [see Fig. 1(b)], the energy-resolved RS distribution shown in Fig. 1(c) displays modulations of the PL intensity, indicating underlying density oscillations. Indeed, the time-resolved RS distribution, shown in Fig. 1(d), reveals the spatial density oscillations, while the KS distribution shows that the majority of the polaritons occupy the  $k \sim 0$  state [38].

It is important to stress that the images in Figs. 1(c) and 1(d) are accumulated over millions of condensation realisations. The persistent density modulations mean that the dynamics recurs despite the stochastic nature of the condensate formation in every experimental realisation [37]. This recurrence is due to a significant wedge of our microcavity (effective linear potential) [36] oriented along the diagonal  $x$ - $y$  direction, as evidenced by the off-centered RS image in Fig. 1(a) and the tilted low-energy tail of the energy-resolved RS distribution in Fig. 1(c).

To analyze the observed oscillations, we perform time-resolved tomography on the RS  $n_r(x, y, t)$  and KS  $n_k(k_x, k_y, t)$  density distributions [38]. The snapshots at different times [Figs. 2(a), 2(b)] reveal “sloshing” of the condensate along the cavity wedge (see Supplemental Movie [38]). When most of the polaritons are on one side of the trap,  $n_k$  is centered at  $k \approx 0$  [right panels in Figs. 2(a), 2(b)], corresponding to zero average momentum at the classical turning point of the confining potential. When the  $n_r$  is symmetric,  $n_k$  is off-centered [left panels in Figs. 2(a), 2(b)], corresponding to a large average momentum. This harmonic motion is summarized in Figs. 2(c), 2(d), where the expectation values of position  $\langle x \rangle$  and momentum  $\langle \hbar k \rangle$ , are calculated as  $\langle x \rangle = \int x n_r dx dy / \int n_r dx dy$  and  $\langle k \rangle = \int k n_k dk_x dk_y / \int n_k dk_x dk_y$ . The behavior of the expectation values is in excellent agreement with the Ehrenfest’s theorem of quantum mechanics:  $m(d\langle x \rangle/dt) = \langle \hbar k_x \rangle$ , as demonstrated by the

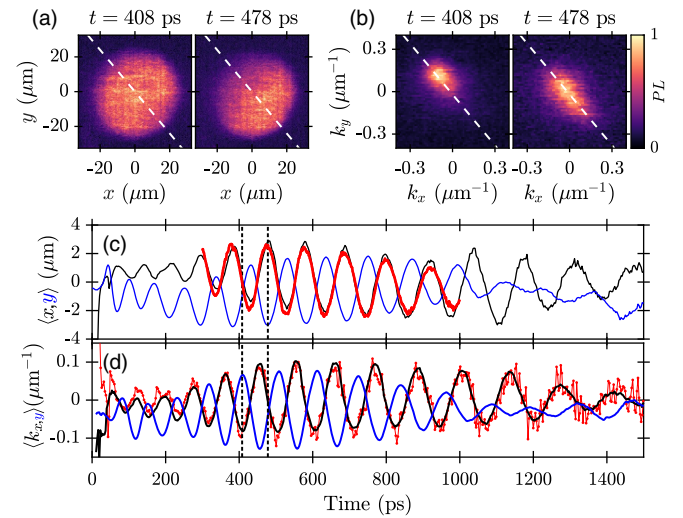


FIG. 2. Snapshots of (a) RS and (b) KS condensate density distributions at two different times. Dashed lines show the direction of the microcavity wedge. Time-evolution of the average (c) position  $\langle x \rangle$  (black),  $\langle y \rangle$  (blue) and (d) momentum  $\langle \hbar k_x \rangle$  (black),  $\langle \hbar k_y \rangle$  (blue), extracted from the condensate density distributions. Red line in (c) corresponds to the time-dependent amplitude  $w(t)$  of the dipole mode in Fig. 3(b). Red dots in (d) correspond to  $(m/\hbar)d\langle x \rangle/dt$  calculated from (c). Vertical dashed lines correspond to the snapshots in (a),(b).

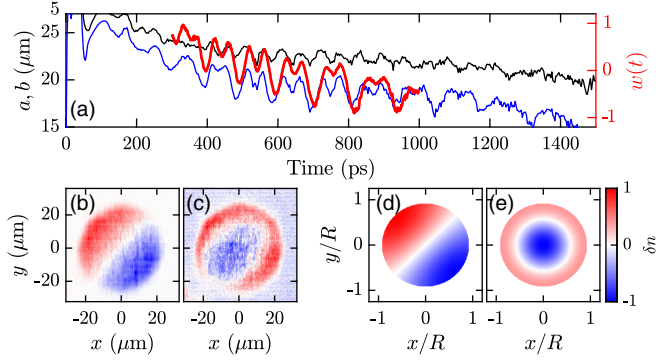


FIG. 3. Time-evolution of the semiaxes of the ellipse  $a$  (black) and  $b$  (blue) fitted to the condensate density distribution  $n_r(x, y, t)$ . (b),(c) Normal modes extracted by PCA. Red line in (a) corresponds to the amplitude  $w(t)$  (in arbitrary units) of the PCA mode shown in (c). The amplitude  $w(t)$  for the mode in (b) is shown in Fig. 2(c). (d) Dipole and (e) breathing modes calculated from theory.

overlap of  $\langle k_x \rangle$  (solid black line) and  $(m/\hbar)d\langle x \rangle/dt$  (red dots) in Fig. 2(d). Here,  $m$  is the polariton effective mass at a near-zero energy detuning between the exciton and the cavity photon [38].

The condensate density distribution obtained from the experimental RS images indicates that the box trap has an elliptical rather than circular cross section, with an aspect ratio of 1.2. By fitting the edges of the density distribution with an ellipse with semi-axes  $a, b$  [38], we extract the time evolution of the condensate width shown in Fig. 3(a). The oscillation frequency is clearly distinct from the average position or momentum in Figs. 2(c), 2(d). To identify the normal modes of this oscillation, we employ a principal component analysis (PCA). This model-free statistical analysis tool [9,40,41] allows us to extract the spatial profile of the normal modes (principal components)  $\mathcal{P}_c(x, y)$  and their time-dependent amplitudes  $w_c(t)$  from the density  $n_r(x, y, t) = \overline{n_r(x, y)} + \sum_{c=1}^{N_t} w_c(t) \mathcal{P}_c(x, y)$ , where  $\overline{n_r(x, y)}$  is the time average [38]. The PCA reveals two dominant modes shown in Figs. 3(b), 3(c). The respective amplitudes  $w(t)$ , marked by the red line in Figs. 2(c) and 3(a), match the oscillations of the average position and width of the condensate.

The observed dynamics can be understood as a result of collective excitations of the polariton condensate. In the homogeneous, steady-state regime, polariton decay and interaction with the reservoir strongly modifies the dispersion of excitations at low momenta  $k < k_s$  [27,28], where  $k_s$  is determined by the polariton lifetime [38]. For  $k > k_s$ , the dispersion recovers its sonic character, i.e.,  $\omega \approx ck$ , where  $c$  is the speed of sound. The long polariton lifetime ( $\sim 200$  ps) in our experiment results in a very small  $k_s \approx 0.01 \mu\text{m}^{-1}$ , an order of magnitude smaller than the momenta corresponding to the observed oscillations. For the sake of simplicity and in the absence of a better suited

theory, we analyze the oscillations in the framework of equilibrium quantum hydrodynamics.

The total condensate density can be approximated by  $n(x, y, t) = n_0(x, y) + \delta n(x, y, t)$  where  $n_0$  is the ground state density and  $\delta n \ll n$  is the density of excitations. This approximation is validated by the low occupation of the normal modes relative to the condensate,  $\delta N/N \sim 0.1$ , extracted from PCA. In a round box trap of radius  $R$ , the density  $n_0$  has a flat-top profile in the Thomas-Fermi limit [35]. Neglecting the sharp edges of  $n_0$ , the hydrodynamic equation for the collective excitations can be written as [54]  $\omega^2 \delta n = -c^2 \nabla^2 \delta n$ . The wave equation is subject to the boundary conditions  $\nabla \delta n = 0$  at the edge ( $r = R$ ) and the continuity condition in the azimuthal direction. The normal modes have the form:

$$\delta n_{l,m} \propto J_m \left( \frac{q_{l,m} r}{R} \right) e^{im\phi}, \quad (1)$$

where  $J_m$  is the Bessel function of the 1st kind and  $q_{l,m}$  is the  $l$ th root of its derivative  $J'_m$ . The indices  $l, m$  denote the radial nodes and the orbital angular momentum of the mode, respectively, resulting in the dispersion

$$\omega_{l,m} = cq_{l,m}/R. \quad (2)$$

Of particular interest are the dipole ( $l = 1, m = \pm 1$ ) and the breathing ( $l = 1, m = 0$ ) modes with the spatial profiles shown in Figs. 3(d), 3(e) (see the Supplemental Material [38] for other modes) and frequencies  $\omega_D \approx 1.84c/R$  and  $\omega_B \approx 3.83c/R$ , respectively. The dipole mode is a “vortex”-like center-of-mass motion around the trap center but the reduced symmetry of the elliptical trap results in oscillations along the short (long) axis of the trap at a slightly higher (lower) frequency. The breathing mode shown in Fig. 3(e) becomes a mixture of the monopole and quadrupole modes, with a pronounced oscillation of the condensate width that does not affect its center of mass. The dominant modes extracted by PCA [Figs. 3(b), 3(c)] are now readily identified as the dipole and breathing modes by comparison with Figs. 3(d), 3(e), and by matching the respective amplitudes with the observed oscillations in Figs. 2(c) and 3(a).

A remarkable advantage of a box trap is the dependence of the mode frequencies on the speed of sound, Eq. (2), which for a 2D quantum gas is a function of its thermodynamic properties and the interaction strength [2,55]. In order to analyze the frequencies of the two dominant oscillations, we perform a time-frequency analysis of the oscillation signals presented in Figs. 2(c) and 3(a) using a wavelet synchrosqueezed transform [42]. Figure 4(a) shows the two extracted down-chirped frequencies (see the Supplemental Material [38] for more details). The low-frequency mode is extracted from  $\langle x, y \rangle$  and is therefore

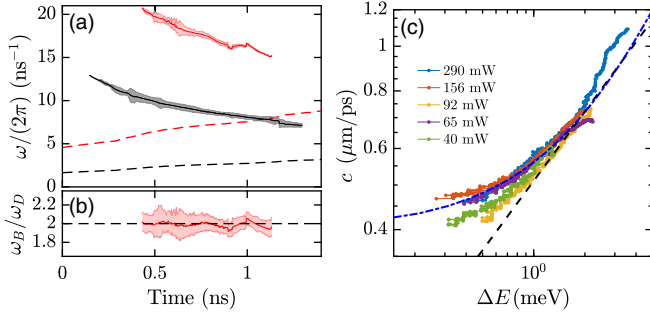


FIG. 4. Measurement of the speed of sound. (a) Frequency of the dipole (black) and breathing (red) modes. Black dashed line corresponds to the noninteracting dipole (breathing) frequency  $\omega_D^{\text{sp}}$  ( $\omega_B^{\text{sp}}$ ). (b) Ratio of the breathing and dipole frequencies  $\omega_B/\omega_D$ . Shaded areas in (a),(b) correspond to the width of the extracted peak from the time-frequency analysis. (c) Speed of sound extracted from the dipole frequency as function of blueshift,  $\Delta E$ , for different excitation powers above the condensation threshold,  $P_{\text{th}} \approx 10.5$  mW. The black dashed line ( $c = c_B/3$ ) and the blue dash-dotted line ( $c = c_0 + c_1\Delta E$ , where  $c_0 = 0.4 \mu\text{m ps}^{-1}$  and  $c_1 = 0.16 \mu\text{m ps}^{-1} \text{meV}^{-1}$ ) are guides to the eye corresponding to the expected square-root dependence and the observed linear dependence, respectively.

due to the dipole oscillation, while the high-frequency component is extracted from  $a$ ,  $b$  and is due to the breathing oscillation.

The observed frequencies can be compared to those in a noninteracting, single-particle (sp) limit, where the oscillation is due to the linear superposition of the ground and excited states with either  $m = 1$  (dipole) or  $m = 0$  (breathing). These frequencies are plotted as dashed lines in Fig. 4(a) (see the Supplemental Material [38] for more details), where we estimate the trap radius  $R$  from the running average of the measured Thomas-Fermi condensate width. Clearly, the observed frequencies are much higher than the noninteracting case, the ratio  $\omega_B/\omega_D \approx 2$ , shown in Fig. 4(b), is smaller than the noninteracting limit of  $\omega_B^{\text{sp}}/\omega_D^{\text{sp}} \approx 2.7$ , and the frequency chirp is reversed. Thus, the observed oscillation is collective in nature, in contrast to previously observed nonequilibrium motion of polaritons in a ring [56].

The breathing mode is a compressional mode of the 2D quantum gas, sensitive to the equation of state [55]. For a 2D weakly interacting Bose gas in an elliptical box trap with the aspect ratio  $a/b \approx 1.2$ , one expects  $\omega_B/\omega_D \approx 2$  [38]. The ratio  $\omega_B/\omega_D \approx 2.0$  observed in the polariton condensate [Fig. 4(b)] therefore suggests that it behaves as a weakly interacting 2D Bose gas in a box trap.

The dipole mode can be used to measure the speed of sound using the dispersion law, Eq. (2), and assuming that the condensate is in a quasisteady state. This is a reasonable assumption because the condensate decays slowly, so that there are  $> 10$  oscillations per lifetime. At zero temperature and with negligible quantum depletion, the speed of sound

should be equal to the Bogoliubov sound  $c_B = \sqrt{gn/m}$ , where  $\mu = gn$  is the condensate interaction energy,  $g$  is the polariton-polariton interaction strength,  $n$  is the polariton density, and  $m$  is the effective mass. The interaction energy in our experiment can be inferred from the instantaneous blueshift  $\Delta E$  of the condensate energy [Fig. 1(b)], provided that it arises only due to the polariton-polariton interaction [35].

Figure 4(c) presents the measured speed of sound,  $c$ , as a function of the blueshift,  $\Delta E$ , for different excitation powers, where the blueshift is measured with respect to the polariton energy at  $k = 0$  in the low-density limit [38]. As expected, the speed of sound decreases with the diminishing interaction energy (i.e., with time) and its general behavior is independent of the excitation power, which only determines the initial polariton density and blueshift. The results for different trap sizes and effective masses [38] show that, at early times,  $c$  is independent of the trap size and decreases with increasing effective mass. At large blueshifts (or early times),  $c(\Delta E)$  follows the predicted square-root law but with  $c \approx c_B/3$ . Furthermore, when  $\Delta E \lesssim 1$  meV, this dependence deviates from the square-root law and becomes linear  $c \propto \Delta E$ .

The discrepancy between the measured and predicted speed of sound at large blueshifts can be attributed to the presence of the reservoir. In contrast to our previous work [35], here the reservoir is not fully depleted, as evidenced by the slow decay of the condensate PL [38]. Therefore the polariton-reservoir interaction contributes to the measured blueshift, i.e.,  $\Delta E = g(n + |X|^{-2}n_R)$ , where  $n_R$  is the reservoir density, and  $|X|^2$  is the excitonic Hopfield coefficient. Consequently,  $c_B = \sqrt{gn/m} < \sqrt{\Delta E/m}$ . Given the value for the interaction strength at nearzero detuning ( $|X|^2 = 1/2$ ) [33,35], we can estimate the ratio of densities to be  $n_R/n \approx 4$  at early times and  $n_R/n \approx 1.5$  at later times [38]. The latter value agrees with previous measurements under off resonant [33] and resonant [32] CW excitation conditions. Therefore, the observed deviation from the square-root scaling at later times could indicate that both the reservoir and condensate densities approach a stationary state.

Although the oscillation frequencies  $\omega_{B,D}$  and their ratio are in good agreement with the conservative theory, the damping of the excitations is the consequence of driven-dissipative and finite-temperature effects. The damping rates estimated from the data in Figs. 2(d) and 3(a) [38] are  $\gamma_D \sim 1 \text{ ns}^{-1}$  for the dipole mode and  $\gamma_B \sim 2 \text{ ns}^{-1}$  for the breathing mode, resulting in a  $Q$  factor  $Q = \omega/\gamma \sim 60$ . The damping can be due to different mechanisms. Decay and driven thermalization of polaritons leads to damping of the excitations [27–30] with the rate determined by the polariton lifetime and the stimulated scattering rate from the reservoir to the condensate [38]. While the latter is not known, a reasonable estimate [38] leads to the damping

rates on the order of  $\text{ns}^{-1}$ , which are similar to the rates observed in the experiment. Similar rates can also arise from excitations of the excitonic reservoir [27–30] (see the Supplemental Material [38]). Furthermore, the excitations can be damped by scattering with lattice phonons [57], which results in effective polariton energy relaxation [35,58,59]. A similar relaxation process has been shown to damp condensate oscillations in conservative (cold atomic) systems [60]. However, these effects cannot fully account for the observed dependence of the damping rates on the momentum. Interaction with uncondensed, thermal polaritons, which are observable in high quality samples and have an effective temperature of  $T \sim 10$  K [33,61], such that  $k_B T \sim gn \gg \hbar\omega_{B,D}$ , can lead to momentum-dependent Landau damping [3,4,62]. The measured  $Q$  factors of the two modes are similar to those reported in previous studies of Landau damping of collective oscillations in a conservative 2D Bose gas in the collisionless regime [1,3,4]. Indeed, our condensate is in the interaction-driven collisionless rather than the hydrodynamic regime [3] because the effective collision frequency [43]  $\Omega \sim 0.1\text{--}1 \text{ ns}^{-1}$  is much smaller than  $\omega_{B,D}$  [38].

*Conclusion.*—We have observed collective oscillations of a polariton condensate in a box trap. The oscillations are dominated by the dipole and breathing modes, with the ratio of frequencies well described by a model of 2D weakly interacting bosons. The speed of sound determined from the dipole frequency is lower than the Bogoliubov sound, assuming the condensate blueshift is only due to polariton-polariton interaction. This discrepancy points to the significant influence of the reservoir.

Our future work will focus on selective excitation of collective modes by pulsed perturbation of a steady-state condensate. This will allow us to relate the dispersion of excitations [33] to the measured speed of sound, determine the momentum dependence of the damping rates, and identify the dominant damping mechanism.

Our study paves the way for further investigations of the collective excitations of polariton condensates, which are essential for better understanding of the driven-dissipative and finite temperature effects [3,4,63] on the superfluidity of 2D nonequilibrium systems. Precise measurements of the breathing mode frequency can lead to experiments on quantum corrections beyond the mean-field approximation [6,7], and enable tests of a crossover between the quantum phases of polariton systems.

This work was supported by the Australian Research Council (ARC) through the Centre of Excellence Grant No. CE170100039. M.P. acknowledges support by the Foundation for Polish Science (FNP) in the START programme and National Science Center in Poland, Grant No. 2018/30/E/ST7/00648. The work at Pittsburgh and Princeton was supported by the US National Science Foundation Grant No. DMR-2004570.

\*eliezer.estrecho@anu.edu.au

†elena.ostrovskaya@anu.edu.au

‡Present address: Department of Experimental Physics, Wrocław University of Science and Technology, Wyb. Wyspiańskiego 27, 50-370 Wrocław, Poland.

§Present address: National Renewable Energy Lab, Golden, Colorado 80401, USA.

- [1] J. L. Ville, R. Saint-Jalm, É. Le Cerf, M. Aidelsburger, S. Nascimbène, J. Dalibard, and J. Beugnon, Sound Propagation in a Uniform Superfluid Two-Dimensional Bose Gas, *Phys. Rev. Lett.* **121**, 145301 (2018).
- [2] M. Ota and S. Stringari, Second sound in a two-dimensional Bose gas: From the weakly to the strongly interacting regime, *Phys. Rev. A* **97**, 033604 (2018).
- [3] M. Ota, F. Larcher, F. Dalfovo, L. Pitaevskii, N. P. Proukakis, and S. Stringari, Collisionless Sound in a Uniform Two-Dimensional Bose Gas, *Phys. Rev. Lett.* **121**, 145302 (2018).
- [4] A. Cappellaro, F. Toigo, and L. Salasnich, Collisionless dynamics in two-dimensional bosonic gases, *Phys. Rev. A* **98**, 043605 (2018).
- [5] M. Bohlen, L. Sobirey, N. Luick, H. Biss, T. Enss, T. Lompe, and H. Moritz, Sound Propagation and Quantum-Limited Damping in a Two-Dimensional Fermi Gas, *Phys. Rev. Lett.* **124**, 240403 (2020).
- [6] T. Peppler, P. Dyke, M. Zamorano, I. Herrera, S. Hoinka, and C. J. Vale, Quantum Anomaly and 2D-3D Crossover in Strongly Interacting Fermi Gases, *Phys. Rev. Lett.* **121**, 120402 (2018).
- [7] M. Holten, L. Bayha, A. C. Klein, P. A. Murthy, P. M. Preiss, and S. Jochim, Anomalous Breaking of Scale Invariance in a Two-Dimensional Fermi Gas, *Phys. Rev. Lett.* **121**, 120401 (2018).
- [8] L. Tanzi, S. M. Rocuzzo, E. Lucioni, F. Famà, A. Fioretti, C. Gabbanini, G. Modugno, A. Recati, and S. Stringari, Supersolid symmetry breaking from compressional oscillations in a dipolar quantum gas, *Nature (London)* **574**, 382 (2019).
- [9] G. Natale, R. M. W. van Bijnen, A. Patscheider, D. Petter, M. J. Mark, L. Chomaz, and F. Ferlaino, Excitation Spectrum of a Trapped Dipolar Supersolid and Its Experimental Evidence, *Phys. Rev. Lett.* **123**, 050402 (2019).
- [10] M. Guo, F. Böttcher, J. Hertkorn, J.-N. Schmidt, M. Wenzel, H. P. Büchler, T. Langen, and T. Pfau, The low-energy Goldstone mode in a trapped dipolar supersolid, *Nature (London)* **574**, 386 (2019).
- [11] H. Deng, G. Weihs, C. Santori, J. Bloch, and Y. Yamamoto, Condensation of semiconductor microcavity exciton polaritons, *Science* **298**, 199 (2002).
- [12] J. Kasprzak, M. Richard, S. Kundermann, A. Baas, P. Jeambrun, J. M. J. Keeling, F. M. Marchetti, M. H. Szymńska, R. André, J. L. Staehli, V. Savona, P. B. Littlewood, B. Deveaud, and L. S. Dang, Bose-Einstein condensation of exciton polaritons, *Nature (London)* **443**, 409 (2006).
- [13] R. Balili, V. Hartwell, D. Snoke, L. Pfeiffer, and K. West, Bose-Einstein condensation of microcavity polaritons in a trap, *Science* **316**, 1007 (2007).
- [14] H. Deng, H. Haug, and Y. Yamamoto, Exciton-polariton Bose-Einstein condensation, *Rev. Mod. Phys.* **82**, 1489 (2010).

- [15] I. Carusotto and C. Ciuti, Quantum fluids of light, *Rev. Mod. Phys.* **85**, 299 (2013).
- [16] T. Byrnes, N. Y. Kim, and Y. Yamamoto, Exciton-polariton condensates, *Nat. Phys.* **10**, 803 (2014).
- [17] G. Roumpos, M. Lohse, W. H. Nitsche, J. Keeling, M. H. Szymańska, P. B. Littlewood, A. Löffler, S. Höfling, L. Worschech, A. Forchel, and Y. Yamamoto, Power-law decay of the spatial correlation function in exciton-polariton condensates, *Proc. Natl. Acad. Sci. U.S.A.* **109**, 6467 (2012).
- [18] W. H. Nitsche, N. Y. Kim, G. Roumpos, C. Schneider, M. Kamp, S. Höfling, A. Forchel, and Y. Yamamoto, Algebraic order and the Berezinskii-Kosterlitz-Thouless transition in an exciton-polariton gas, *Phys. Rev. B* **90**, 205430 (2014).
- [19] D. Caputo, D. Ballarini, G. Dagvadorj, C. Sánchez Muñoz, M. De Giorgi, L. Dominici, K. West, L. N. Pfeiffer, G. Gigli, F. P. Laussy, M. H. Szymańska, and D. Sanvitto, Topological order and thermal equilibrium in polariton condensates, *Nat. Mater.* **17**, 145 (2018).
- [20] J. Keeling, P. R. Eastham, M. H. Szymańska, and P. B. Littlewood, BCS-BEC crossover in a system of microcavity polaritons, *Phys. Rev. B* **72**, 115320 (2005).
- [21] T. Byrnes, T. Horikiri, N. Ishida, and Y. Yamamoto, BCS Wave-Function Approach to the BEC-BCS Crossover of Exciton-Polariton Condensates, *Phys. Rev. Lett.* **105**, 186402 (2010).
- [22] J. Hu, Z. Wang, S. Kim, H. Deng, S. Brodbeck, C. Schneider, S. Höfling, N. H. Kwong, and R. Binder, Signatures of a Bardeen-Cooper-Schrieffer Polariton Laser, *Phys. Rev. X* **11**, 011018 (2021).
- [23] R. T. Jiggins, J. Keeling, and M. H. Szymańska, Coherently driven microcavity-polaritons and the question of superfluidity, *Nat. Commun.* **9**, 4062 (2018).
- [24] G. Nardin, G. Grosso, Y. Léger, B. Pietka, F. Morier-Genoud, and B. Deveaud-Plédran, Hydrodynamic nucleation of quantized vortex pairs in a polariton quantum fluid, *Nat. Phys.* **7**, 635 (2011).
- [25] A. Amo, J. Lefrère, S. Pigeon, C. Adrados, C. Ciuti, I. Carusotto, R. Houdré, E. Giacobino, and A. Bramati, Superfluidity of polaritons in semiconductor microcavities, *Nat. Phys.* **5**, 805 (2009).
- [26] G. Lerario, A. Fieramosca, F. Barachati, D. Ballarini, K. S. Daskalakis, L. Dominici, M. De Giorgi, S. A. Maier, G. Gigli, S. Kéna-Cohen, and D. Sanvitto, Room-temperature superfluidity in a polariton condensate, *Nat. Phys.* **13**, 837 (2017).
- [27] J. Keeling, P. R. Eastham, M. H. Szymańska, and P. B. Littlewood, Polariton Condensation with Localized Excitons and Propagating Photons, *Phys. Rev. Lett.* **93**, 226403 (2004).
- [28] M. Wouters and I. Carusotto, Excitations in a Nonequilibrium Bose-Einstein Condensate of Exciton Polaritons, *Phys. Rev. Lett.* **99**, 140402 (2007).
- [29] T. Byrnes, T. Horikiri, N. Ishida, M. Fraser, and Y. Yamamoto, Negative Bogoliubov dispersion in exciton-polariton condensates, *Phys. Rev. B* **85**, 075130 (2012).
- [30] L. A. Smirnov, D. A. Smirnova, E. A. Ostrovskaya, and Yu. S. Kivshar, Dynamics and stability of dark solitons in exciton-polariton condensates, *Phys. Rev. B* **89**, 235310 (2014).
- [31] S. Utsunomiya, L. Tian, G. Roumpos, C. W. Lai, N. Kumada, T. Fujisawa, M. Kuwata-Gonokami, A. Löffler, S. Höfling, A. Forchel, and Y. Yamamoto, Observation of Bogoliubov excitations in exciton-polariton condensates, *Nat. Phys.* **4**, 700 (2008).
- [32] P. Stepanov, I. Amelio, J.-G. Rousset, J. Bloch, A. Lemaître, A. Amo, A. Minguzzi, I. Carusotto, and M. Richard, Dispersion relation of the collective excitations in a resonantly driven polariton fluid, *Nat. Commun.* **10**, 3869 (2019).
- [33] M. Pieczarka, E. Estrecho, M. Boozarjmehr, O. Bleu, M. Mark, K. West, L. N. Pfeiffer, D. W. Snoke, J. Levinsen, M. M. Parish, A. G. Truscott, and E. A. Ostrovskaya, Observation of quantum depletion in a non-equilibrium exciton-polariton condensate, *Nat. Commun.* **11**, 429 (2020).
- [34] D. Ballarini, D. Caputo, G. Dagvadorj, R. Jiggins, M. De Giorgi, L. Dominici, K. West, L. N. Pfeiffer, G. Gigli, M. H. Szymańska, and D. Sanvitto, Directional Goldstone waves in polariton condensates close to equilibrium, *Nat. Commun.* **11**, 217 (2020).
- [35] E. Estrecho, T. Gao, N. Bobrovska, D. Comber-Todd, M. D. Fraser, M. Steger, K. West, L. N. Pfeiffer, J. Levinsen, M. M. Parish, T. C. H. Liew, M. Matuszewski, D. W. Snoke, A. G. Truscott, and E. A. Ostrovskaya, Direct measurement of polariton-polariton interaction strength in the Thomas-Fermi regime of exciton-polariton condensation, *Phys. Rev. B* **100**, 035306 (2019).
- [36] B. Nelsen, G. Liu, M. Steger, D. W. Snoke, R. Balili, K. West, and L. Pfeiffer, Dissipationless Flow and Sharp Threshold of a Polariton Condensate with Long Lifetime, Dissipationless Flow and Sharp Threshold of a Polariton Condensate with Long Lifetime, *Phys. Rev. X* **3**, 041015 (2013).
- [37] E. Estrecho, T. Gao, N. Bobrovska, M. D. Fraser, M. Steger, L. Pfeiffer, K. West, T. C. H. Liew, M. Matuszewski, D. W. Snoke, A. G. Truscott, and E. A. Ostrovskaya, Single-shot condensation of exciton polaritons and the hole burning effect, *Nat. Commun.* **9**, 2944 (2018).
- [38] See Supplemental Material at <http://link.aps.org/supplemental/10.1103/PhysRevLett.126.075301> for additional details of the experiment, theoretical modeling, principal component analysis and time-frequency analysis, discussion of the damping rates, and the estimate of the reservoir to condensate ratio, which includes Refs. [1,3,4,28–30,32,35,39–53]. Supplemental Movie Supplemental\_Movie.avi shows experimentally recorded temporal dynamics of condensate oscillations in real and momentum space.
- [39] C. Antón, T. C. H. Liew, G. Tosi, M. D. Martín, T. Gao, Z. Hatzopoulos, P. S. Eldridge, and P. G. Savvidis, and L. Viña, Energy relaxation of exciton-polariton condensates in quasi-one-dimensional microcavities, *Phys. Rev. B* **88**, 035313 (2013).
- [40] S. R. Segal, Q. Diot, E. A. Cornell, A. A. Zozulya, and D. Z. Anderson, Revealing buried information: Statistical processing techniques for ultracold-gas image analysis, *Phys. Rev. A* **81**, 053601 (2010).
- [41] R. Dubessy, C. De Rossi, T. Badr, L. Longchambon, and H. Perrin, Imaging the collective excitations of an ultracold gas using statistical correlations, *New J. Phys.* **16**, 122001 (2014).

- [42] I. Daubechies, Y. Wang, and H.-T. Wu, ConceFT: Concentration of frequency and time via a multitapered synchrosqueezed transform, *Phil. Trans. R. Soc. A* **374**, 20150193 (2016).
- [43] D. S. Petrov and G. V. Shlyapnikov, Interatomic collisions in a tightly confined Bose gas, *Phys. Rev. A* **64**, 012706 (2001).
- [44] M. Pieczarka, M. Boozarjmehr, E. Estrecho, Y. Yoon, M. Steger, K. West, L. N. Pfeiffer, K. A. Nelson, D. W. Snoke, A. G. Truscott, and E. A. Ostrovskaya, Effect of optically-induced potential on the energy of trapped exciton-polaritons below the condensation threshold, *Phys. Rev. B* **100**, 085301 (2019).
- [45] P. W. M. Blom, P. J. Van Hall, C. Smit, J. P. Cuypers, and J. H. Wolter, Selective Exciton Formation in thin GaAsAl<sub>x</sub>Ga<sub>1-x</sub>As Quantum Wells, *Phys. Rev. Lett.* **71**, 3878 (1993).
- [46] G. Bacher, C. Hartmann, H. Schweizer, and H. Nickel, Modulated energy relaxation of photoexcited carriers into the excitonic ground state in shallow In<sub>x</sub>Ga<sub>1-x</sub>AsGaAs quantum wells, *Solid State Commun.* **95**, 15 (1995).
- [47] J. Kovac, H. Schweizer, M. H. Pilkuhn, and H. Nickel, Influence of the kinetic energy of electrons on the formation of excitons in a shallow In<sub>x</sub>Ga<sub>1-x</sub>As/GaAs quantum well, *Phys. Rev. B* **54**, 13440 (1996).
- [48] K. Winkler, O. A. Egorov, I. G. Savenko, X. Ma, E. Estrecho, T. Gao, S. Müller, M. Kamp, T. C. H. Liew, E. A. Ostrovskaya, S. Höfling, and C. Schneider, Collective state transitions of exciton-polaritons loaded into a periodic potential, *Phys. Rev. B* **93**, 121303(R) (2016).
- [49] X. Antoine and R. Duboscq, GPELab, a Matlab toolbox to solve Gross-Pitaevskii equations I: Computation of stationary solutions, *Comput. Phys. Commun.* **185**, 2969 (2014).
- [50] X. Antoine and R. Duboscq, GPELab, a Matlab toolbox to solve Gross-Pitaevskii equations II: Dynamics and stochastic simulations, *Comput. Phys. Commun.* **193**, 95 (2015).
- [51] I. Jolliffe, *Principal Component Analysis* (Springer, New York, 2011).
- [52] MATLAB version 9.6.0.1150989 (R2019a).
- [53] M.-C. Chung and A. B. Bhattacharjee, Damping in 2D and 3D dilute Bose gases, *New J. Phys.* **11**, 123012 (2009).
- [54] S. Stringari, Collective Excitations of a Trapped Bose-Condensed Gas, *Phys. Rev. Lett.* **77**, 2360 (1996).
- [55] G. De Rosi and S. Stringari, Collective oscillations of a trapped quantum gas in low dimensions, *Phys. Rev. A* **92**, 053617 (2015).
- [56] S. Mukherjee, D. M. Myers, R. G. Lena, B. Ozden, J. Beaumariage, Z. Sun, M. Steger, L. N. Pfeiffer, K. West, A. J. Daley, and D. W. Snoke, Observation of nonequilibrium motion and equilibration in polariton rings, *Phys. Rev. B* **100**, 245304 (2019).
- [57] M. Wouters, Energy relaxation in the mean-field description of polariton condensates, *New J. Phys.* **14**, 075020 (2012).
- [58] E. Wertz, A. Amo, D. D. Solnyshkov, L. Ferrier, T. C. H. Liew, D. Sanvitto, P. Senellart, I. Sagnes, A. Lemaître, A. V. Kavokin, G. Malpuech, and J. Bloch, Propagation and Amplification Dynamics of 1D Polariton Condensates, *Phys. Rev. Lett.* **109**, 216404 (2012).
- [59] N. Bobrovska, E. A. Ostrovskaya, and M. Matuszewski, Stability and spatial coherence of nonresonantly pumped exciton-polariton condensates, *Phys. Rev. B* **90**, 205304 (2014).
- [60] S. Choi, S. A. Morgan, and K. Burnett, Phenomenological damping in trapped atomic Bose-Einstein condensates, *Phys. Rev. A* **57**, 4057 (1998).
- [61] Y. Sun, P. Wen, Y. Yoon, G. Liu, M. Steger, L. N. Pfeiffer, K. West, D. W. Snoke, and K. A. Nelson, Bose-Einstein Condensation of Long-Lifetime Polaritons in Thermal Equilibrium, *Phys. Rev. Lett.* **118**, 016602 (2017).
- [62] S. Giorgini, Damping in dilute Bose gases: A mean-field approach, *Phys. Rev. A* **57**, 2949 (1998).
- [63] M. Wouters and I. Carusotto, Superfluidity and Critical Velocities in Nonequilibrium Bose-Einstein Condensates, *Phys. Rev. Lett.* **105**, 020602 (2010).